



# Evaluation and preparation of $\text{Li}_{1+x-y}\text{Nb}_{1-x-3y}\text{Ti}_{x+4y}\text{O}_3$ solid solution with superstructure as new phosphor

Hiroyuki Hayashi<sup>a,\*</sup>, Hiromi Nakano<sup>b</sup>

<sup>a</sup> KRI, Inc. Device Process Unit, Nano-Device Research Laboratory, Kyoto research Park, 134, Chudoji Minami-machi, Shimogyo-ku, Kyoto 600-8813, Japan

<sup>b</sup> Faculty of Science and Technology, Ryukoku University, Seta, Otsu, Shiga 520-2194, Japan

## ARTICLE INFO

### Article history:

Received 2 June 2009

Received in revised form 19 April 2010

Accepted 24 April 2010

Available online 4 May 2010

### Keywords:

Superstructure

$\text{LiNbO}_3$

$\text{TiO}_2$

Phosphor

$\text{Eu}_2\text{O}_3$

## ABSTRACT

New red phosphors have been investigated in this study with europium as an activator added to  $\text{Li}_{1+x-y}\text{Nb}_{1-x-3y}\text{Ti}_{x+4y}\text{O}_3$  (LNT) solid solutions with an M Phase superstructure. The photo-luminescence intensity of LNT:Eu solid solutions was dependent on the levels of both the Eu doping and the  $\text{TiO}_2$  content, and was superior to that of  $\text{LiNbO}_3$ :Eu. LNT:Eu solid solutions with 2.5 wt.%  $\text{Eu}_2\text{O}_3$  showed the highest performance in this work, and maximum intensity was observed when the  $\text{TiO}_2$  content of LNT:Eu solid solutions was 10 mol.%. Structural analysis by XRD and HREM showed that in these new phosphors the M Phase superstructure was affected by the doping, with the periodicity of the superstructure becoming wider and more random.

© 2010 Elsevier B.V. All rights reserved.

## 1. Introduction

$\text{Li}_{1+x-y}\text{Nb}_{1-x-3y}\text{Ti}_{x+4y}\text{O}_3$  ( $0.11 \leq x \leq 0.33$ ,  $0 \leq y \leq 0.09$ ) (hereafter LNT) forms solid solutions with a superstructure, known as the M Phase, in the  $\text{Li}_2\text{O}-\text{Nb}_2\text{O}_5-\text{TiO}_2$  ternary system. Since the discovery of this M Phase by Villafuerte-Castrejon et al. [1,2], both its crystal structure [3–6] and the applications of Phase M [7–9] have been studied. LNT solid solutions of M Phase have a hexagonal subcell similar to the unit cell of  $\text{LiNbO}_3$ , which belongs to the trigonal system ( $R3c$ ), and has lattice constants of  $a = 0.5148$  nm,  $c = 1.3863$  nm. The superstructure of LNT solid solutions was identified using HREM as having layer-like domains [4,5], where stacking faults are inserted parallel to the  $c$  axis in the  $\text{LiNbO}_3$  structure. The stacking faults have a rock-salt structure and the dimension of the domain along the  $c$  axis based on a  $\text{LiNbO}_3$ -like subcell has been controlled by  $\text{TiO}_2$  content and sintering temperature [5]. The period of superstructure was shown to decrease with increasing  $\text{TiO}_2$  content.

Eu doped  $\text{LiNbO}_3$  thin films showing stress luminescence have been reported [10] and recently,  $\text{LiNbO}_3$  (hereafter LN) as a host crystal for phosphors has been studied [11]. The ionic radius of Eu is sufficiently larger than that of Li or Nb and if not controlled via

sintering temperature,  $\text{Nb}_2\text{O}_5$  reacts with  $\text{Eu}_2\text{O}_3$  to form  $\text{EuNbO}_4$  [11].

Fluorescent thin films with a superstructure formed by CVD have been researched, and it was reported that the luminescence was superior to that of a thin film with normal structure [6]. These superstructures consist of periodic layering where each layer has the same crystal structure, but the lattice constants and compositions of individual layers are different. Distortion of the structure introduced by differences in the two lattice constants was inserted periodically in the microstructure of the solid solution. This leads to improved properties when compared to the base compound due to the strain energy. However, in order to prepare them, special equipment is required such as CVD for semiconductor manufacturing equipment. In addition the applications of such superstructured materials are limited in the thin film field.

On the other hand, M Phase solid solutions have a self-organized super lattice which can be prepared in a commercial furnace. The super-periodicity of M Phase solid solutions can be controlled by the composition and sintering temperature, and employing this spontaneous superstructure it is possible to prepare by materials by a commercial powder mixing method and sol-gel method [5]. Therefore M Phase has the advantage that the sintered bodies can be prepared as single crystal [12,13], bulk body [5], powder and thin film [12,13].

In this work we have prepared Eu doped LN and Eu doped LNT solid solutions of M Phase. In terms of improving the luminescence property of LNT:Eu, the relationship between Eu additive amount or

\* Corresponding author.

E-mail addresses: [h-hayasi@kri-inc.jp](mailto:h-hayasi@kri-inc.jp) (H. Hayashi), [hiromi@rins.ryukoku.ac.jp](mailto:hiromi@rins.ryukoku.ac.jp) (H. Nakano).

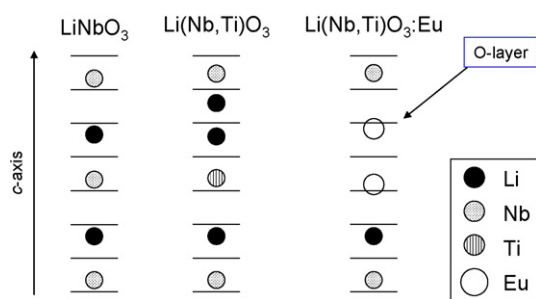


**Fig. 1.** The schematic of structure of  $\text{LiNbO}_3$ , LNT solid solution and Eu doped LNT solution.

Ti displacement amount and the luminescence intensity of LNT:Eu has been clarified.

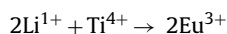
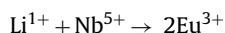
## 2. Experimental procedure

The compositions of LNT:Eu solid solutions in this work were  $0 \leq x \leq 0.33$  and  $y = 0$ . Starting materials of  $\text{Li}_2\text{CO}_3$  (Wako),  $\text{Nb}_2\text{O}_5$  (Wako, 3N),  $\text{TiO}_2$  (Wako) and  $\text{Eu}_2\text{O}_3$  (Wako, 3N) were prepared by dry mixing. The mixed powder was sintered at both  $1000^\circ\text{C}$  (3 h) and  $1120^\circ\text{C}$  (10 h) in air. The  $\text{Eu}_2\text{O}_3$  content was varied from 1 to 5 wt.%.

The excitation and emission spectra of the samples were measured by a spectrometer FP-6500 model (JASCO). XRD was carried out using a RINT2500 (Rigaku Co. Ltd.) at 50 kV and 200 mA. Structural images and selected area electron diffraction patterns (SAED) were observed by high-resolution TEM (JEM-3000F, JEOL Co. Ltd.) at 300 kV. Chemical composition was analyzed using a HREM, which makes it possible to provide electron probes with at half maximum of  $\sim 0.5$  nm, and also with sufficiently high current for a point analysis by energy dispersive X-ray spectroscopy (EDS) (Noran Instruments Voyager III).

## 3. Results and discussions

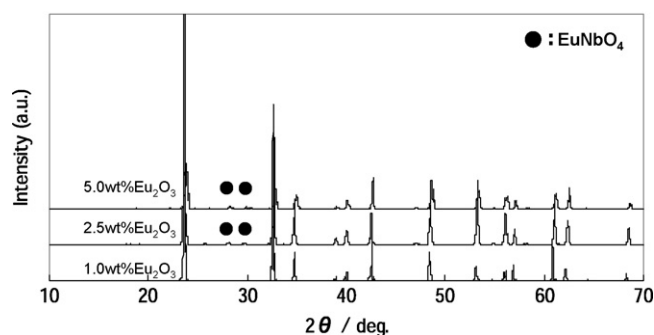
The identification of phase and crystal structure analysis of Eu doped LNT solid solutions were observed by XRD. The microstructure of LNT solid solutions of Phase M have a  $\text{LiNbO}_3$ -like subcell structure and the structure of stacking faults periodically inserted in the LNT crystal is a rock-salt structure of  $\text{Li}_2\text{TiO}_3$  [5]. The Ti mainly exists in the stacking faults of the superstructure. When considering the charge balance when Eu is doped into LNT, two types of the displacement are possible.



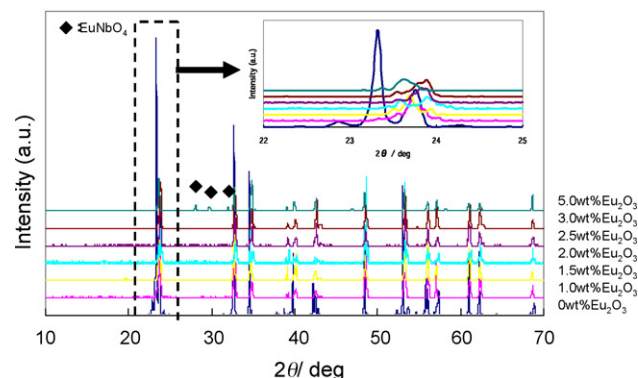
It was considered that the Eu can therefore exist in both the  $\text{LiNbO}_3$ -like subcell and the stacking faults. Fig. 1 shows the schematic of structure of  $\text{LiNbO}_3$ , LNT solid solution and Eu doped LNT solution. Consequently, in these doped materials there is the possibility that  $\text{LiNbO}_3$  and  $\text{Li}_2\text{TiO}_3$  remains as a secondary phase, or unreacted  $\text{Eu}_2\text{O}_3$  may be found in the product. There is also a danger that  $\text{EuNbO}_4$  and  $\text{EuTiO}_3$  may be produced. XRD spectra of the Eu doped LN samples are shown in Fig. 2. It can be seen that the prepared samples have the  $\text{LiNbO}_3$  structure and  $\text{EuNbO}_4$  is observed in both 2.5 and 5%  $\text{Eu}_2\text{O}_3$  doped samples. The amount of  $\text{EuNbO}_4$  in the product increased with increasing additive amount of  $\text{Eu}_2\text{O}_3$ .

Fig. 3 shows the XRD patterns of LNT solid solutions with 10 mol.%  $\text{TiO}_2$  and different amounts of  $\text{Eu}_2\text{O}_3$  additions. In these samples no  $\text{EuNbO}_4$  was observed for  $\text{Eu}_2\text{O}_3$  additions up to 3%. However, for the 5 wt.%  $\text{Eu}_2\text{O}_3$  additive the excess Eu reacted with Nb to form  $\text{EuNbO}_4$ . The differences in the amount of  $\text{Eu}_2\text{O}_3$  that is required before the  $\text{EuNbO}_4$  phase is observed indicates that the solid solubility limit of Eu for LNT solid solutions is greater than that of LN.

The superstructure normally observed in LNT solid solutions results can be observed as a splitting of the (0 1 2) peak of the  $\text{LiNbO}_3$



**Fig. 2.** XRD patterns of LN:Eu.  $\text{Eu}_2\text{O}_3$  contents are 1.0, 2.5 and 5.0 wt.%.



**Fig. 3.** XRD patterns of LNT:Eu solid solution (10 mol.%  $\text{TiO}_2$ ) added various contents of  $\text{Eu}_2\text{O}_3$ . Focused patterns of  $2\theta = 22\text{--}25^\circ$  was inserted. Diamond symbol showed  $\text{EuNbO}_4$ .

structure at around  $2\theta = 23$ , where the peak can be resolved into 4 components. Increasing separation of the split peaks relates to a decrease in the super-periodicity of the LNT solid solution. The insert in Fig. 3 shows a close up of this region of the spectra. It can be seen that the LNT sample with no Eu shows peak splitting, but this is not observed in the Eu doped samples, indicating that the superstructure formation was obstructed by Eu doping.

It is thought that the Eu doping decreases the Ti diffusion rate and inhibits the introduction of the stacking faults. This is confirmed from structural observations by HREM and an analysis of distribution of Eu and Ti by TEM-EDS. The 10 mol.%  $\text{TiO}_2$  LNT solid solutions with 0 and 2.5 wt.% Eu doping are shown in Fig. 3. It was observed that LNT solid solution with no Eu doping (Fig. 4a) had a periodic structure whereas the Eu doped sample (Fig. 4b), contained stacking faults that were discontinuous resulting in a loss of periodicity. The results of TEM-EDS analysis shown in Table 1 show that Ti and Eu elements are concentrated more in the stacking faults than in the  $\text{LiNbO}_3$ -like subcell. It is thought that Eu doping results in the destruction of the rock-salt structure of the stacking faults.

The luminescence of the LNT solid solutions with Eu as activator were measured by excitation at  $\lambda = 380$  nm. The emission spectra presented in Fig 5a show that the main emission peak of Eu doped LNT solid solutions was at  $\lambda = 625$  nm. An additional peak

**Table 1**  
Compositions of LNT:Eu solid solution (10 mol.%  $\text{TiO}_2$ ) analyzed by TEM-EDS.

	Additive		Non-additive
	Subcell	Stacking faults	Subcell + stacking faults
Nb	91.78	87.99	92.17
Ti	6.10	9.23	7.83
Eu	2.12	2.77	0.00

Atom%.

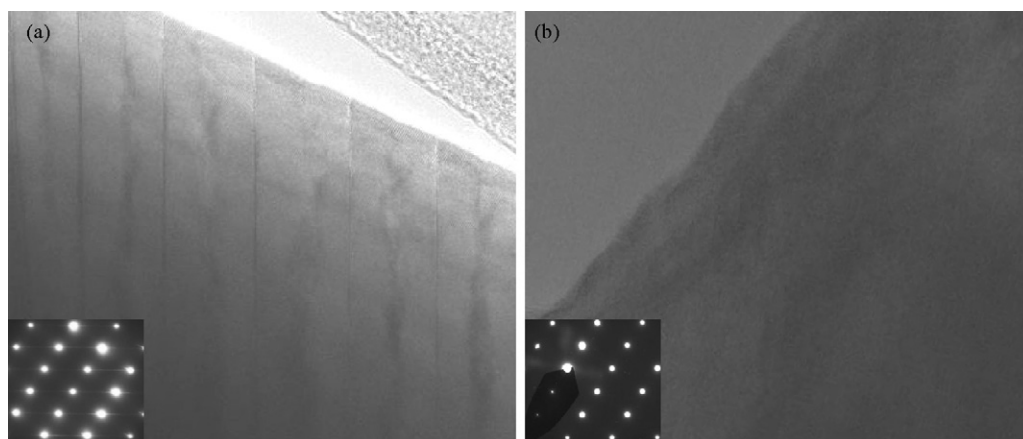


**Fig. 4.** (a) High-resolution TEM photograph and electron diffraction pattern of LNT solid solution (10 mol.% TiO<sub>2</sub>). (b) High-resolution TEM photograph and electron diffraction pattern of Eu doped LNT solid solution (10 mol.% TiO<sub>2</sub>).

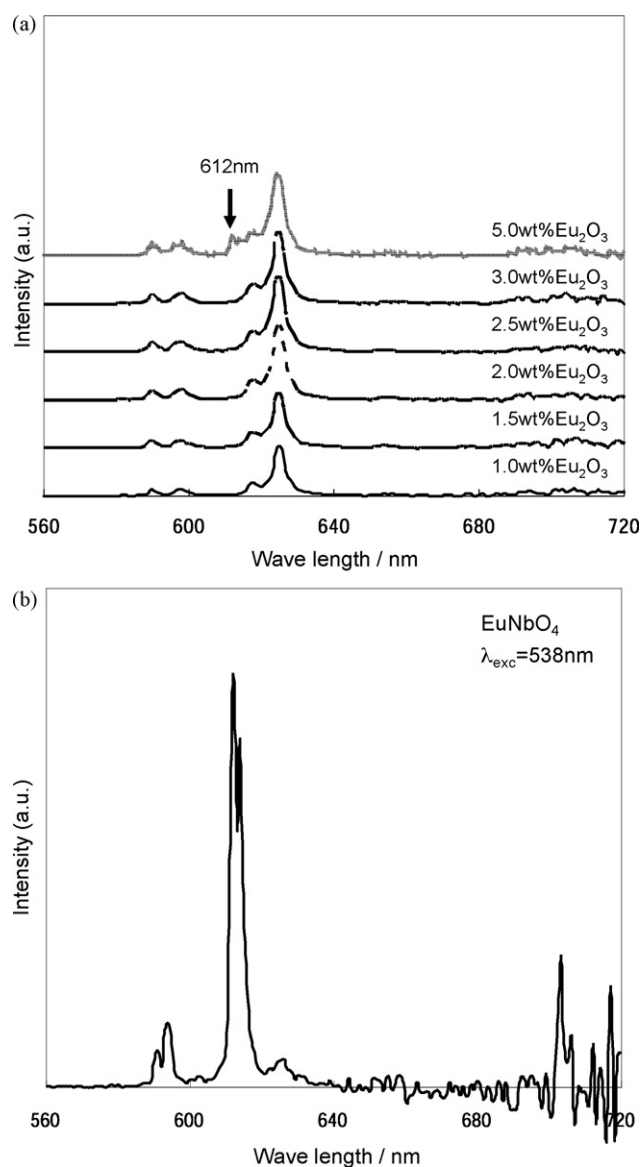


**Fig. 5.** (a) Relationship between emission spectrum excited by  $\lambda = 380$  nm and Eu<sub>2</sub>O<sub>3</sub> content for LNT:Eu solid solution (TiO<sub>2</sub> = 10 mol.%). (b) Emission spectra of EuNbO<sub>4</sub> (excited by  $\lambda = 538$  nm).

at  $\lambda = 612$  nm was observed only for the sample doped with 5 wt.% Eu<sub>2</sub>O<sub>3</sub>. Fig. 5b shows the emission spectra of pure EuNbO<sub>4</sub> where it can be seen that this peak is associated with the EuNbO<sub>4</sub> phase. The emission spectra results therefore support the XRD results where the EuNbO<sub>4</sub> phase was observed only for the 5 wt.% Eu doped sample.

Fig. 6a shows the excitation spectra of the Eu doped LNT solid solutions. All of the spectra show three absorption peaks at  $\lambda = 398$  nm, 468 nm and 541 nm. For Eu contents up to 3%, which all emitted at  $\lambda = 625$  nm the intensity of the 398 nm excitation peak showed the highest intensity. The 5 wt.% Eu<sub>2</sub>O<sub>3</sub> doped LNT solid solutions showed two different spectra. The EuNbO<sub>4</sub> as a secondary phase was identified by XRD, and the luminescence of this EuNbO<sub>4</sub> was observed. For the 5% doped sample which emitted at  $\lambda = 612$  nm, the strongest absorption peak was the one at  $\lambda = 538$  nm. This is again related to the presence of the EuNbO<sub>4</sub> phase as indicated by Fig. 6b which shows excitation spectra for EuNbO<sub>4</sub>. When the samples were excited at  $\lambda = 398$  nm there was no difference in the emission spectra of the samples with different Eu contents as shown in Fig. 7. The luminescence intensity of LNT samples with different amounts of Eu additive when changing the TiO<sub>2</sub> content (varying composition of LNT solid solutions) is shown in Fig. 8. These samples were excited at  $\lambda = 398$  nm. The luminescence intensities of LNT solid solutions:Eu were higher than that of LN:Eu, and for all Eu contents the maximum intensity was observed at 10 mol.% TiO<sub>2</sub>. For LN:Eu samples the highest intensity was observed for the 2.0 wt.% Eu sample, and for the LNT:Eu samples the highest intensity was obtained with 2.5 wt.% doping. The relationship between the compositions and emission spectra of the LNT:Eu 2.5 wt.% is given in Fig. 9. For TiO<sub>2</sub> contents up to 10 mol.% there is a clear separation of peaks at  $\lambda = 618$  nm and  $\lambda = 625$  nm. For higher TiO<sub>2</sub> contents there was broadening of the peak at  $\lambda = 618$  nm until it becomes absorbed by the peak at  $\lambda = 625$  nm. It is thought that this is due to a change in the electron state associated with the change in crystal structure symmetry.

Comparing the luminescence of LNT:Eu phosphor with commercial phosphors of blue, green and yellow were shown in Fig. 10. It was thought Eu doped LNT phosphor prepared in this work was adapted to a phosphor for a white LED.

#### 4. Summary

Eu doped LiNbO<sub>3</sub> and Eu doped LNT solid solutions were prepared and it was found that for small amounts of a LiNbO<sub>3</sub> type structure was observed. For the LN materials, Eu<sub>2</sub>O<sub>3</sub> amounts greater than 2.0 wt.%, resulted in a secondary EuNbO<sub>4</sub> phase whilst

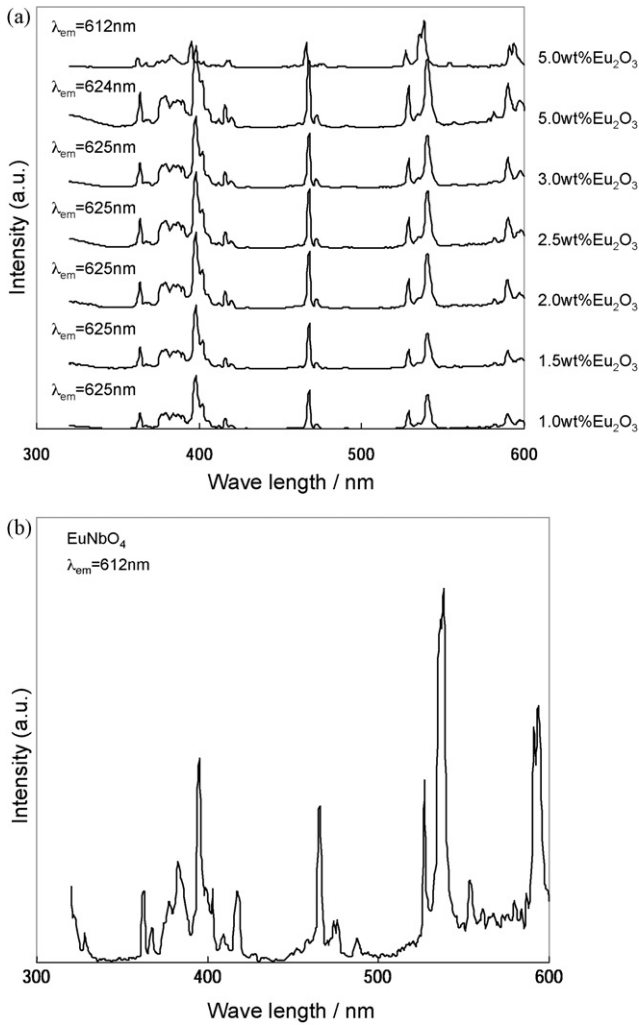


Fig. 6. (a) Variation of excitation spectrum of LNT:Eu solid solution (TiO<sub>2</sub> = 10 mol.%) for Eu<sub>2</sub>O<sub>3</sub> contents. (b) Emission spectra of EuNbO<sub>4</sub> (emission by λ = 612 nm).

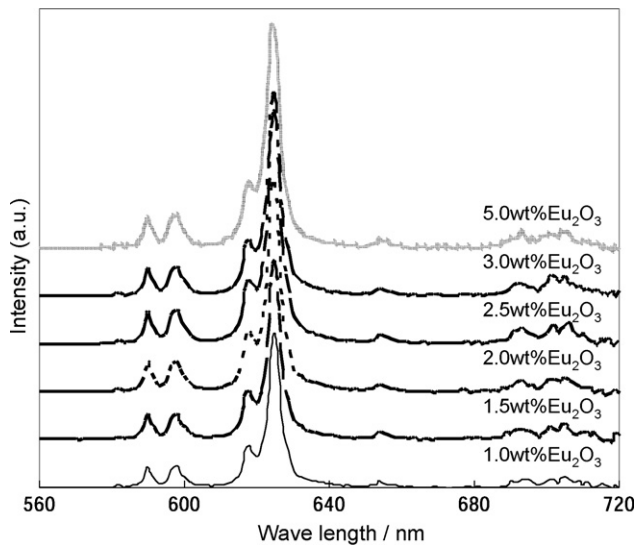


Fig. 7. Relationship between emission spectrum excited by λ = 398 nm and Eu<sub>2</sub>O<sub>3</sub> content.

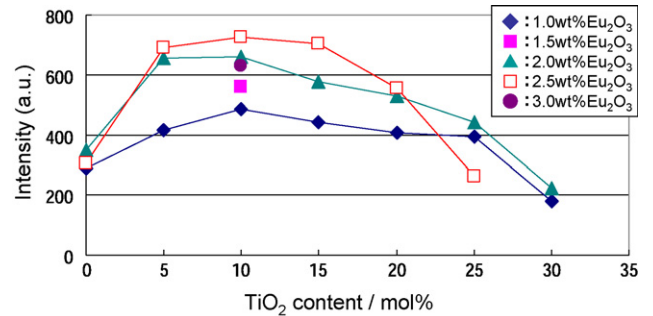


Fig. 8. Relationship between TiO<sub>2</sub> content of LNT:Eu solid solutions and photoluminescence intensity.

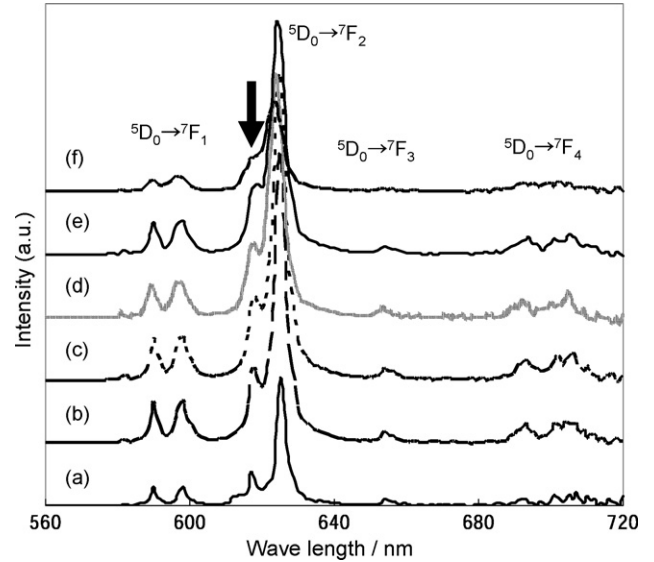


Fig. 9. Emission spectrum excited by λ = 398 nm of LNT:Eu solid solutions. Eu<sub>2</sub>O<sub>3</sub> was added at 2.5 wt.%. TiO<sub>2</sub> content is (a) 0 mol.%, (b) 5 mol.%, (c) 10 mol.%, (d) 15 mol.%, (e) 20 mol.% and (f) 25 mol.%.

in the LNT solid solutions this was not observed for Eu<sub>2</sub>O<sub>3</sub> amounts up to 3.0 wt.%. This suggests that solubility of Eu is greater in the LNT compositions. When TiO<sub>2</sub> and Eu<sub>2</sub>O<sub>3</sub> were added to LiNbO<sub>3</sub>, the luminescence intensity of the solid solutions markedly improved over that of the LN:Eu. In terms of luminescence intensity it was observed that the most suitable Eu additive density was 2.0 wt.% in LiNbO<sub>3</sub> and 2.5 wt.% in the LNT solid solutions, and it was confirmed

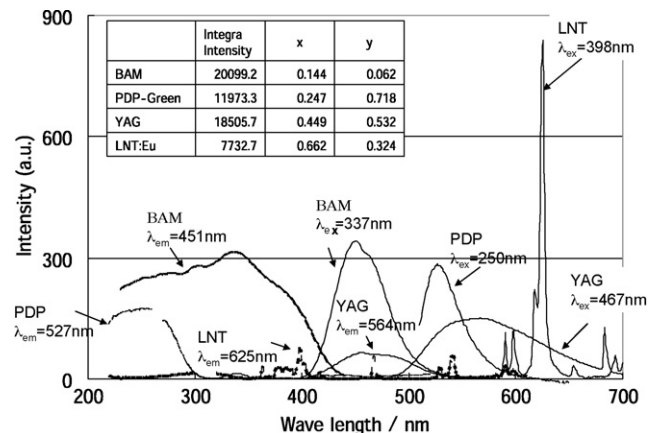


Fig. 10. The emission and excitation spectra of LNT:Eu and commercial phosphors. BAM: blue, Green: green and YAG: yellow.

that the intensity of LNT solid solutions was twice as large as that of  $\text{LiNbO}_3$ . In LNT solid solutions, the most suitable  $\text{TiO}_2$  content was 10 mol.%. LNT solid solutions with 10 mol.%  $\text{TiO}_2$  usually have a superstructure, but it was discovered that Eu doping prevented the formation of such a superstructure in LNT solid solutions. XRD measurements showed that no such structure was observed in the Eu doped LNT solid solution at the same level of  $\text{TiO}_2$ , and the destruction of the periodicity of the M Phase superstructure was confirmed by HREM. It is concluded that the increase in luminescence intensity does not arise from the superstructure, but is related to the most suitable density of Ti and Eu in the LNT solid solutions.

### Acknowledgement

The authors gratefully acknowledge Dr. Mark I. Jones (Auckland University, New Zealand) for helpful discussions and for checking the manuscript, and Mr. Mutsuo Masuda (KRI Inc.) for helpful advice on emission characteristics.

### References

- [1] M.E. Villafuerte-Castrejon, J.A. Gracia, E. Cisneros, R. Valenzuela, A.R. West, *Trans. J. Brit. Ceram. Soc.* 83 (1984) 143.
- [2] M.E. Villafuerte-Castrejon, A. Aragon-Pina, R. Valenzuela, A.R. West, *J. Solid State Ceram.* 71 (1987) 103.
- [3] R.I. Smith, A.R. West, *Mater. Res. Bull.* 27 (1992) 277.
- [4] H. Hayashi, H. Nakano, K. Suzumura, K. Urabe, A.R. West, *Forth Ceram. Soc.* 2 (1995) 391.
- [5] H. Hayashi, K. Urabe, K. Niihara, *Key Eng. Mater.* 161–163 (1999) 501.
- [6] H. Koinuma, Y. Matsumoto, Y. Shimomura, N. Kujima, JP 3,582,010 B2 (2004).
- [7] A.Y. Borisevich, S.V. Kalinin, D.A. Bonnell, P.K. Davies, *J. Mater. Res.* 16 (2001) 329.
- [8] A.Y. Borisevich, P.K. Davies, *J. Am. Ceram. Soc.* 85 (2002) 573.
- [9] Y. Yamamoto, H. Hayashi, T. Sekino, T. Nakayama, T. Kondo, M. Wada, T. Adachi, K. Niihara, *Mater. Res. Innovations* 7 (2003) 74–79.
- [10] A.A. Kaplyanskii, S. Kapphan, A.B. Kutsenko, K. Polgar, A.P. Skvortsov, *Tech. Phys. Lett.* 33 (2007) 337.
- [11] L.A. Souza, Y. Messaddeq, S.J.L. Ribeiro, C. Fredericci, F. Lanciotti Jr., P.S. Pizani, *Quim. Nova* 25 (2002) 1067.
- [12] Y. Yamamoto, T. Sekino, H. Hayashi, T. Nakayama, T. Kusunose, K. Niihara, *Mater. Lett.* 57 (2003) 2702.
- [13] Y. Yamamoto, T. Sekino, H.T. Kusunose, T. Nakayama, K. Niihara, *Mater. Integr.* 17 (2004) 10.